

## Tunable magnetization damping in transition metal ternary alloys

S. Ingvarsson<sup>a)</sup>

Department of Physics, Brown University, Providence, Rhode Island 02912  
and IBM Research Division, T. J. Watson Research Center, Yorktown Heights, New York 10598

Gang Xiao

Department of Physics, Brown University, Providence, Rhode Island 02912

S. S. P. Parkin

IBM Research Division, Almaden Research Center, Almaden, California 95120

R. H. Koch

IBM Research Division, T. J. Watson Research Center, Yorktown Heights, New York 10598

(Received 23 July 2004; accepted 11 October 2004)

We show that magnetization damping in Permalloy,  $\text{Ni}_{80}\text{Fe}_{20}$ , can be enhanced sufficiently to reduce postswitching magnetization precession to an acceptable level by alloying with the transition metal Os (osmium). The damping increases monotonically upon raising the Os concentration in Permalloy, at least up to 9% of Os. Other effects of alloying with Os are suppression of magnetization and enhancement of in-plane anisotropy. Magnetization damping also increases significantly upon alloying with the five other transition metals included in this study ( $4d$  elements: Nb, Ru, Rh;  $5d$  elements: Ta, Pt) but never as strongly as with Os. © 2004 American Institute of Physics.  
[DOI: 10.1063/1.1828232]

Magnetic tunnel junctions (MTJ) are presently under intense development for use in magnetic random access memory (MRAM).<sup>1,2</sup> In a slightly modified configuration from the MRAM they can be made extremely sensitive to changes in magnetic field.<sup>3,4</sup> Such microscopic magnetic field sensors are employed in magnetic recording read heads, readily resolving magnetic bits smaller than  $0.1\ \mu\text{m}$ . Alternatively MTJ sensors can be scanned along surfaces making a magnetic microscope with great spatial resolution.<sup>5,6</sup> The functionality of these devices is based on a change in resistance of the MTJ in response to a change in relative magnetic orientation of a “free layer” with respect to a magnetically “pinned layer.” These layers are separated (and exchange decoupled) by an insulating oxide tunnel barrier. Essential to the high-speed functionality of these devices is the swift response of the free layer to the applied field. It must switch between equilibrium positions defined by the magnetic field conditions, with minimal “unnecessary” magnetization motion. Excessive magnetization precession during the device’s relaxation toward equilibrium can cause serious delays. In the MRAM case the unwanted precession shows up as oscillations in the resistance *after* switching has taken place, often referred to as magnetic “ringing.”<sup>7</sup> In some cases this even leads to uncertainty of the final state of the device for a given applied field.

An example of these adverse affects of magnetization precession is displayed in Fig. 1, measured on a hexagonally shaped MRAM cell with in-plane extremal dimensions of  $0.28$  and  $0.84\ \mu\text{m}$ . The MRAM has two equilibrium positions, with parallel (low resistance) and antiparallel magnetization (high resistance). The figure displays a critical switching curve, extracted from two experiments, one switching the MRAM from parallel to antiparallel configuration (going from right to left in the figure, determining the left boundary of the green area, where the free layer is re-

versed), and the other switching from antiparallel to parallel (left to right, resolving the right boundary of the green area). In both experiments the initial state is indicated by a green color, regardless of whether the configuration is parallel or antiparallel. The resistance scale depicts resistance *relative to the initial state*. The switching was carried out with magnetic field pulses of varying strength,  $4\ \text{ns}$  in duration with the rise of the easy-axis pulse delayed by  $2\ \text{ns}$  with respect to the rising edge of the hard-axis pulse. These experiments correspond to measuring the Stoner–Wolfarth astroid by applying short magnetic field pulses. Two features in particular set the critical switching curves measured with short field pulses apart from those measured with slowly varying fields. First are the wide openings at the top and bottom around zero easy-axis field. Second are the individual unsuccessful switching attempts where the MRAM refused to switch even

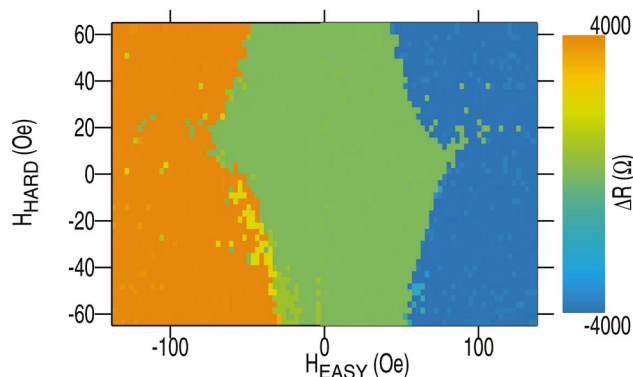


FIG. 1. (Color) Critical switching curve for a hexagon-shaped MRAM cell with dimensions  $0.28$  by  $0.84\ \mu\text{m}$ . The initial state is indicated by a green color, regardless of whether the configuration is parallel or antiparallel. The resistance scale depicts resistance *relative to the initial state*. Thus going from right to left (left to right) in the figure the resistance increases (decreases) as the configuration switches at the left (right) green boundary. The switching was carried out with magnetic field pulses of varying strength,  $4\ \text{ns}$  in duration with the rise of the easy-axis pulse delayed by  $2\ \text{ns}$  with respect to the rising edge of the hard-axis pulse.

<sup>a)</sup>Present address: Icelandic Technological Institute, Keldnaholt, IS-112 Reykjavik, Iceland; electronic mail: sthi@iti.is

though the applied fields lie far beyond the continuous part of the curve. We refer to these anomalous events as “freckles.” Freckles are stochastic in the sense that they are not entirely reproducible, but do appear in the same general area of two-dimensional field space. They disappear upon lengthening the field pulses, but appear for different combinations of nanosecond scale pulse lengths with different delay times between hard- and easy-axis pulses. They are believed to be caused by precession of the magnetic moment after the free layer magnetization has been switched. If the precession amplitude is large a small perturbation can force the MRAM from the switched state back to the original state.

Efforts to reduce postswitching precession in thin films suitable for MRAM elements include shaping of the magnetic field pulses employed to switch the devices and using so-called precessional switching.<sup>8–10</sup> In precessional switching a perpendicular field pulse is applied to the magnetic layer and the natural precession of the material is used to aid the switching. These methods have allowed “ringing-free” switching at speeds an order of magnitude faster than the time constant of natural damping in the material. For obvious reasons these developments do not help in sensor applications, in which case one seldom has much control over the field being sensed, neither its magnitude nor direction.

An alternative approach in contending undesirable magnetic precession is to increase the magnetization damping in the material. This helps the magnetic moment reach equilibrium sooner, thus reducing the risk of thermal excitation to a different equilibrium position. Increased damping can be achieved either by modifying the bulk of the material (e.g., by alloying,<sup>11,12</sup> ion irradiation,<sup>13</sup> or ion implantation), or in the case of thin enough films by modifying their surface (e.g. by introducing certain materials on the surface or by increasing the surface roughness.<sup>14,15</sup>)

We took the latter approach to reducing postswitching precession, i.e., to increase magnetization damping, and present results on the effect of alloying Permalloy, Ni<sub>80</sub>Fe<sub>20</sub> (“Py”) with six different 4*d* and 5*d* transition metals (4*d*: Nb, Ru, Rh; 5*d*: Ta, Os, Pt) keeping the Ni to Fe ratio fixed. We examined the effects these have on the static and dynamic magnetic properties of the materials. Thus we hoped to find a way to increase damping in a manner that appears should lend itself to a greater variety of applications than surface treatment does, and that is generally effective for a wide range of film thickness (or sample size).

We deposited thin films (50 nm thick) of the ternary alloys by dc-magnetron sputtering from ready-made targets with the desired composition. The diluent concentration in the sputter targets was 6%, except for Pt 10% and Rh 5%. The alloy was deposited on top of a buffer layer of 4 nm of Ta sitting on thermally oxidized Si substrates. Ta buffer layers are known to promote small grains and (111) texture in Py.<sup>16</sup> Finally, for protection we used a capping layer of 4 nm thick Ta. Rutherford backscattering measurements on our 6% Os sample confirmed its composition to within 0.5%. Depositions were carried out with an applied magnetic field in the plane of the films, to encourage easy axis growth. Static magnetic properties, i.e., coercive field, in-plane-anisotropy-field, and magnetization were measured with a vibrating sample magnetometer (VSM). The magnetization damping properties were extracted from results of a ferromagnetic resonance measurement by assuming a Gilbert damping term in the Landau–Lifshitz equation,

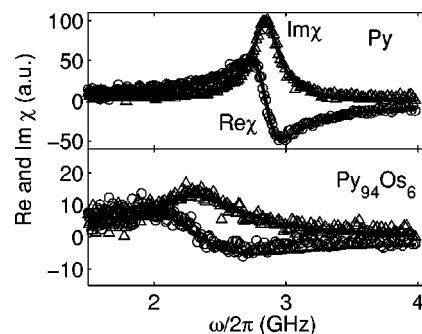


FIG. 2. Results from a ferromagnetic resonance measurement on pure Py (top panel), and an alloy of 94% Py and 6% Os (bottom panel). Each panel displays experimental data for both the real (circles) and the imaginary (triangles) part of the in-plane magnetic susceptibility to an ac-field perpendicular to the easy-axis direction with a 90 Oe dc field applied along the easy axis. Also shown as solid lines, are fits to the data, from which the Gilbert damping ( $\alpha$ ) is obtained.

$$\frac{d\mathbf{M}}{dt} = -\gamma\mathbf{M} \times \mathbf{H}_{\text{eff}} + \frac{\alpha}{M}\mathbf{M} \times \frac{d\mathbf{M}}{dt}, \quad (1)$$

and fitting the complex-valued susceptibility resonance to extract  $\alpha$ , the dimensionless Gilbert damping coefficient.<sup>15,17</sup> Here  $\mathbf{M}$  is magnetization,  $\gamma = g|e|/2mc$  is the gyromagnetic ratio and  $\mathbf{H}_{\text{eff}}$  is the effective magnetic field seen by the magnetization, expressed in terms of the free energy as  $\mathbf{H}_{\text{eff}} = -\nabla_{\mathbf{M}}\mathcal{F}$ .

When magnetization damping increases, i.e.,  $\alpha$  increases in Eq. (1), the ferromagnetic resonance broadens and decreases in amplitude as is the case in Fig. 2. The top panel shows the real and imaginary parts of the complex-valued susceptibility of pure Py around its resonance frequency. The bottom panel displays the corresponding data for Py containing 6% of Os (osmium). The effect of adding Os was so dramatic that the vertical scale in the bottom panel has been blown up and spans only a third of the scale in the top panel. These data correspond to more than a sixfold increase in  $\alpha$  or  $\alpha=0.050$ . The horizontal shift in the resonance towards lower frequency is caused primarily by a decrease in magnetization upon adding Os. The magnetization was measured separately by VSM and included in the fitting procedure. The level of damping obtained goes a long way towards eliminating unwanted magnetization precession. However, in order to convince ourselves that adding Os to Py allows sufficient tunability of the damping we made additional samples with Os concentrations of 3% and 9%, respectively. In Fig. 3 the resulting Gilbert damping (left axis, dots) and magneti-

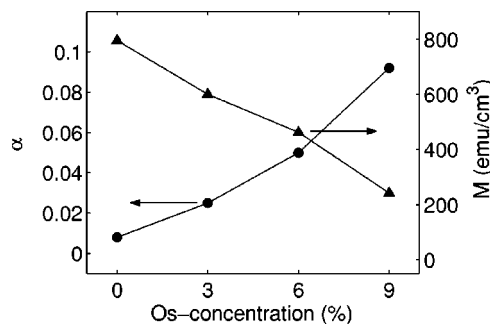


FIG. 3. The effect of Os concentration on both Gilbert damping  $\alpha$  (left axis, dots), and magnetization  $M$  (right axis, filled triangles). The lines are guides for the eye.

TABLE I. Summary of results of Gilbert damping ( $\alpha$ ) and static magnetic properties for alloys of  $\text{Py}_{1-x}\text{X}_x$ , where Py is  $\text{Ni}_{80}\text{Fe}_{20}$  and X is a 4d or 5d transition metal.

X	$\alpha(\times 10^{-3})$	$x(\%)^a$	$M(\text{emu}/\text{cm}^3)$	$H_k(\text{Oe})$	$H_c(\text{Oe})$
		Pure Permalloy ( $\text{Ni}_{80}\text{Fe}_{20}$ )			
	7		796	5.1	1.0
		4d transition metal elements			
Nb	14	6	492	3.0	1.6
Ru	18	6	498	2.7	0.9
Rh	12	5	670	3.9	1.6
		5d transition metal elements			
Ta	16	6	417	2.7	0.8
Os	50	6	462	4.6	2.0
Pt	20	10	649	3.0	4.0

<sup>a</sup>This is the concentration in the sputter target. We did a composition study on the Os-sample, using Rutherford backscattering, and found that the composition of the film was the same as the target composition to within 0.5%. Greater disagreement in the compositions may be expected particularly for larger concentrations of the heaviest elements.

zation values (right axis, triangles) are presented. The Gilbert damping increases and the magnetization decreases, respectively, with increasing Os concentration. The value of  $\alpha$  at 9% Os is 0.092. This corresponds to more than a 12-fold increase compared with pure Py. Raising  $\alpha$  any further than this is likely to result in an overdamped system and an unnecessary slowing down in its dynamic response. In other words, adjustment of the amount of Os in Py within the range shown should *provide sufficient tunability of the magnetization damping to minimize post switching magnetization precession*.

Although some of the other alloys exhibit significant enhancements in  $\alpha$  over the value for pure Py, none are comparable with the Py–Os system. Results for all the alloys are displayed in Table I. Results of VSM-measurements to determine static magnetic properties such as magnetization, in-plane-anisotropy-field ( $H_k$ ), and coercivity ( $H_c$ ) are also included. Note that the VSM-measurements were made on macroscopic films (i.e., unpatterned). Therefore, there is effectively no shape anisotropy in the plane of the film, and the in-plane anisotropy is a measure of average crystalline anisotropy. All the samples have a uniaxial magnetic anisotropy and nice rectangular easy-axis hysteresis loops, some of which are displayed in Fig. 4. From our data there does not appear to be any correlation between the static magnetic properties and  $\alpha$ . It seems that Rh and in particular Pt are

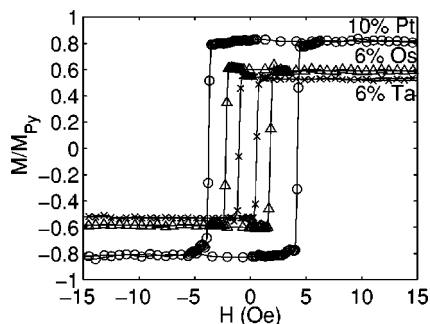


FIG. 4. Hysteresis loops for Py containing 10% Pt, 6% Os, and 6% Ta, respectively.  $H$  is the magnetic field applied parallel to the easy axis. The magnetization is normalized to the saturation magnetization of pure Py.

very “polarizable” in the sense that their addition to Py does not drop the magnetization as much as the other elements do.

Considering the MRAM application in particular, the properties in Table I seem to suggest an alloy of Py and Os as a good choice for a free layer material. However, a most pressing question regarding the use of any of the alloys studied in MRAM elements is: What effect does the alloying have on the spin polarization? Although the levels of spin polarization achieved to date are much larger than needed for MRAM to function well, a significant reduction in polarization may cause problems.<sup>1</sup> Therefore it is of substantial interest to study the spin polarization in these materials.

In summary we have discovered that alloying Permalloy with certain transition metal elements can enhance Gilbert damping significantly. This should help reduce, or even eliminate, superfluous magnetization precession that can adversely affect or hinder many magnetoelectronic applications.

The authors would like to thank K. Pope for the Rutherford backscattering analysis, W. J. Gallagher, T. M. McGuire, and P. L. Trouilloud for many helpful discussions.

<sup>1</sup>S. S. P. Parkin, K. P. Roche, M. G. Samant, P. M. Rice, R. B. Beyers, R. E. Scheuerlein, E. J. O’Sullivan, S. L. Brown, J. Bucchigano, D. W. Abraham, Y. Lu, M. Rooks, P. L. Trouilloud, R. A. Wanner, and W. J. Gallagher, *J. Appl. Phys.* **85**, 5828 (1999).

<sup>2</sup>W. Reohr, H. Honigschmid, R. Robertazzi, D. Gogl, F. Pesavento, S. Lammers, K. Lewis, C. Arndt, Y. Lu, H. Viehmann, R. Scheuerlein, L. K. Wang, P. Trouilloud, S. Parkin, W. Gallagher, and G. Muller, *IEEE Circuits Devices Mag.* **18**, 17 (2002).

<sup>3</sup>X. Liu and G. Xiao, *J. Appl. Phys.* **94**, 6218 (2003).

<sup>4</sup>M. Tondra, J. M. Daughton, C. Nordman, D. Wang, and J. Taylor, *J. Appl. Phys.* **87**, 4679 (2000).

<sup>5</sup>B. D. Schrag and G. Xiao, *Appl. Phys. Lett.* **82**, 3272 (2003).

<sup>6</sup>B. Diény, *J. Magn. Magn. Mater.* **136**, 335 (1994).

<sup>7</sup>R. H. Koch, J. G. Deak, D. W. Abraham, P. L. Trouilloud, R. A. Altman, Y. Lu, W. J. Gallagher, R. E. Scheuerlein, K. P. Roche, and S. S. P. Parkin, *Phys. Rev. Lett.* **81**, 4512 (1998).

<sup>8</sup>T. M. Crawford, P. Kabos, and T. J. Silva, *Appl. Phys. Lett.* **76**, 2113 (2000).

<sup>9</sup>T. Gerrits, H. A. M. van den Berg, J. Hohlfield, L. Bär, and T. Rasing, *Nature (London)* **418**, 509 (2002).

<sup>10</sup>H. W. Schumacher, C. Chappert, P. Crozat, R. C. Sousa, P. P. Freitas, J. Miltat, J. Fassbender, and B. Hillebrands, *Phys. Rev. Lett.* **90**, 017201 (2003).

<sup>11</sup>W. Bailey, P. Kabos, F. Mancoff, and S. Russek, *IEEE Trans. Magn.* **37**, 1749 (2001).

<sup>12</sup>S. Ingvarsson, R. Koch, S. S. P. Parkin, and G. Xiao, U.S. Patent No. 6,452,240 (2002).

<sup>13</sup>S. I. Woods, S. Ingvarsson, J. R. Kirtley, H. F. Hamann, and R. H. Koch, *Appl. Phys. Lett.* **81**, 1267 (2002). Argon ion irradiation was found to affect both magnetization and anisotropy quite significantly.<sup>17</sup> It was also found to affect  $\alpha$ , although not very strongly compared with the effect of alloying. Unfortunately the results were found to be somewhat unpredictable. Due to obvious difficulties with integration of irradiation with the device fabrication processes this method was abandoned.

<sup>14</sup>S. Mizukami, Y. Ando, and T. Miyazaki, *Jpn. J. Appl. Phys., Part 1* **40**, 580 (2001).

<sup>15</sup>S. Ingvarsson, L. Ritchie, X. Y. Liu, G. Xiao, J. C. Slonczewski, P. L. Trouilloud, and R. H. Koch, *Phys. Rev. B* **66**, 214416 (2002). There is an awkward typographical error in Eq. (1). The sign of the second term on the right-hand side should be reversed from  $-$  to  $+$ . This affects neither the analysis nor the results in the paper.

<sup>16</sup>P. Galtier, R. Jerome, and T. Valet, in *Polycrystalline Thin Films: Structure, Texture, Properties and Applications* (Material Research Society, Pittsburgh, 1994), pp. 417–422.

<sup>17</sup>W. F. Brown, *Micromagnetics* (Krieger, Melbourne, FL, 1978).